2011 American Control Conference
on O'Farrell Street, San Francisco, CA, USA
June 29 - July 01, 2011

A Comprehensive Speed Control Model for Human Drivers with Application to Intersection Left Turns

Kazutoshi Nobukawa, Timothy J. Gordon, Michelle A. Barnes and Robert J. Goodsell

Abstract—**This paper presents analysis and modeling of vehicle speed control as demonstrated by human drivers making left turns at intersections. The analysis is based on detailed measurements taken under naturalistic driving conditions. An important application is in the design of future driver assistance systems aimed to reduce intersection collision risk. The model uses the driver's assumed prior estimate of vehicle acceleration based on visual preview information, and unifies estimates of longitudinal acceleration (for braking to rest) and lateral acceleration for negotiating the turn. The relationship between prior acceleration estimates and resulting vehicle accelerations are studied for both stopping and turning events. Closed-loop implementation adopts a nonlinear controller with mode switching functionality. Example simulations show that the model is capable of accurately reproducing measured speed profiles.**

I. Introduction

Intersection accidents are one of the major concerns in traffic safety. Validated computer models are needed to assist with design and performance evaluation of future intersection safety systems, requiring a driver model which is both representative of real-world driving and adaptable to various different driving styles. An accurate speed profile of the turning vehicle is important, since many key conflict metrics for intersection safety analysis are highly sensitive to vehicle speed; these include post-encroachment time (PET) [1], gap time [1, 2] as well as leading and trailing buffers (LB/TB) [3-5]. Therefore, this paper aims to develop a speed control model for this purpose.

Visual and vestibular systems are the most relevant sensory inputs for human drivers [6]. Drivers receive a wide range of information which may affect speed choice, including road geometry (e.g. lane width [7-10] and curve radius [11-13]), and general road conditions [14]. In the scenario of an intersection left turn, and in the absence of collision threats from other vehicles (i.e. a free left turn), the dominant factor is presumed to be lateral acceleration "penalty" for turning too quickly (for safety or comfort) placing an upper limit on the entry speed. Of course, actual thresholds will vary between drivers and change with road surface conditions and other factors.

Visual information is especially important before starting a turn, since there is no direct feedback of lateral acceleration at this stage. Experienced drivers have many occasions to learn associations between visual information available before a turning maneuver and the subsequent experience of whole body acceleration. This motivates the hypothesis that, through experience, human drivers estimate future lateral acceleration, and use this as reference information, $\hat{a}$, to directly control speed during the time interval preceding a turn. Further, since the scenario of braking to rest – say at a stop sign – has similar features, particularly before the brakes are first applied, it is tested whether a similar mechanism might also describe this simpler scenario.

In this paper, an intersection left turn scenario is classified into three stages: *approach*, *turn* and *recovery* stages. The approach stage begins when the vehicle speed starts to reduce on entry to the intersection, initially with the foot lifted from the throttle, and then including braking to control speed before the turn; the turn stage begins at the point where a driving mode switching signal is detected based on the acceleration estimates, and the recovery stage begins when the turn is largely complete, typically when the steering angular velocity is reversed and vehicle speed begins increasing. Two example events are analyzed in this paper as well as two other example for straight braking events to rest; these were chosen for illustration but are typical of many such events chosen so that confounding effects, such as the presence of other vehicles, are absent.

Section II describes the proposed speed control model in detail. In Section III, the prior acceleration estimate $\hat{a}$ is defined and evaluated within relevant scenarios measured in naturalistic driving, so testing whether it is a reasonable candidate reference for speed control. Section IV shows the effect of using $\hat{a}$ as a reference in a closed-loop simulation by including it in a driver model, and Section V gives conclusions.

II. Speed Control Model for Intersection Left Turns

The lateral control of the vehicle is not addressed in this paper. A measured trajectory is used to constrain the steering degree of freedom; this, together with all other measured driving data was obtained from an earlier study [15] – see below. For speed control, a prior acceleration estimate $\hat{a}$ is based in a simple way on the heading angle change between the current vehicle motion and a future reference point,

Manuscript received September 27, 2010.

K. Nobukawa (corresponding author, email: knobukaw@umich.edu) and T. J. Gordon (email: tjgordon@umich.edu) are with the Department of Mechanical Engineering, University of Michigan, Ann Arbor, MI 48109 USA.

M. A. Barnes (email: mbarnes@umich.edu) and R. J. Goodsell (email: bgoodsel@umich.edu) are with the University of Michigan Transportation Research Institute (UMTRI), Ann Arbor, MI 48109 USA.

assuming current speed is maintained. This is shown in Fig. 1 and defined by the following equation:

$$\hat{a} = \frac{U^2}{R} = \frac{2U^2 \sin(|\Delta\psi|/2)}{d} \qquad (1)$$

where U is the current vehicle speed, $\Delta\psi\,(=\psi_{ref}-\psi)$ is the deviation between the current heading angle ψ and desired heading angle ψ_{ref} at the target point Q; $d = |PQ|$ is the instantaneous distance between vehicle and target point. Q is located on the vehicle trajectory near to the start of the turn, and is notionally the gaze point where the driver directs his or her visual attention. During the approach stage, Q is assumed fixed in space, and then at the start of the turn stage Q is to recede along the vehicle trajectory, d then remaining constant. Note that, once P and Q are defined, ψ and ψ_{ref} are obtained from the measured vehicle trajectory.

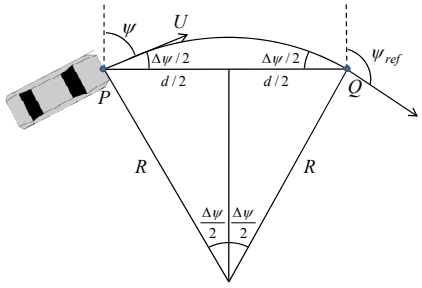

Fig. 1. Geometry for $\hat{a}$ calculation based on circular path and constant speed.

Equation (1) is used for the approach and turn stages, and estimates acceleration based purely on direction change at the current vehicle speed; it requires no complex analysis of vehicle dynamics or of combined slowing and turning. Thus, prediction of future acceleration may be associated with simple visual cues (distance, speed, angles) and it is quite reasonable to expect an experienced driver learns such an association by driving through many intersections and through many continuous curves.

It is worth noting a similarity with the simpler case of speed control for braking to rest; a stopping distance model [16] or equivalently a constant $\dot{\tau}$ strategy [17] have been used previously to describe this case. Here the acceleration estimate is based on uniform deceleration to rest:

$$\hat{a} = \frac{U^2}{2d}\,. \qquad (2)$$

Comparing (1) and (2), the direction change model is equivalent, provided we assume

$$\sin\frac{|\Delta\psi|}{2} = 1/4 \text{ or } |\Delta\psi| \approx 29^\circ\,. \qquad (3)$$

From this, we conjecture a common mechanism for speed control in both straight-line braking and turning at an intersection, both based on prior estimation of future acceleration (longitudinal or lateral). From this, we conjecture a common mechanism for speed control in both straight-line braking and turning at an intersection, both based on prior estimation of future acceleration (longitudinal or lateral). Then for sharp turns ($|\Delta\psi| > 29^\circ$), typical of intersections, the driver can treat the approach as a stopping problem, irrespective of the exact angle of turn. It is therefore efficient to use $\hat{a}_x$ (from (2)) as a reference during the early approach, switching to $\hat{a}_y$ (from (1)) when sufficiently close to the turn.

From this, we assume that driving mode switching, from the approach stage to the turn stage, occurs when the values of $\hat{a}_x$ and $\hat{a}_y$ are equal. The idea is that the driver responds to the lower threat to negotiate the turn - see Section III C. On the other hand, the second switching from the turn stage to recovery stage is found at the point of maximum curvature which roughly corresponds to when the steering angular velocity is reversed. A gaze point for $\hat{a}_x$ is found in the driving data by assuming it coincides with the vehicle position where $\hat{a}_x = a_x$, while the gaze point for $\hat{a}_y$ is selected to be the lane center close to the stop bar of the exit road; ψ_{ref} for $\hat{a}_y$ is defined by the direction of the exit road.

Fig. 2 shows the structure of the overall driver/vehicle combined model for the dynamic simulations, where s is the vehicle position in terms of the path coordinate, U is the speed, a_x is the longitudinal acceleration and $\hat{a}$ is simply the control reference. Since we are only dealing with speed control, the vehicle is represented by a very simple model; the throttle or brakes are applied to the vehicle via an acceleration command u_x , and the vehicle response is found via two integrators, $a_x = u_x$. Detailed dynamics of the vehicle is omitted here, since actual left turn trajectories are directly used to test the presented speed control model. In other words, the purpose of this study is to see whether using the lateral acceleration estimate can reproduce measured speed data.

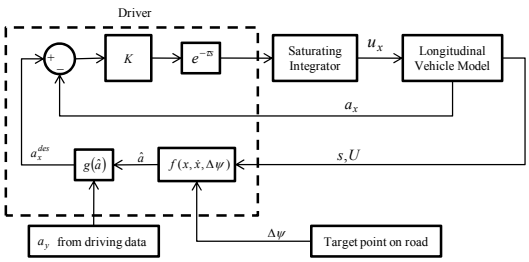

Fig. 2. Block diagram of the closed-loop model.

The driver control model includes an inner loop aimed to track an acceleration reference a_x^{des}. This is essentially an integral control, though with additional saturation limits to avoid unrealistic accelerations and integrator windup. Also, the driver delay ($\tau = 0.2$ s) is included in the inner loop.

The acceleration reference a_x^{des} is derived from $\hat{a}$ via a simple piecewise-linear control function $g(.)$. The model is to apply only in the locality of the intersection, so the driver is assumed to have already lifted the accelerator pedal, generating a gentle coast-down deceleration a_0; this applies until $\hat{a}$ exceeds a certain threshold, at which point a_x^{des} decreases (greater deceleration is demanded) until a second limit on $\hat{a}$ is reached, at which point the demand is saturated. Similar functions are used for the approach and turning stages, though each stage requires separate parameter values in order to match the measured data.

Fig. 3(a) shows $g(.)$ for the approach stage. Here $g(\hat{a}_x) = a_0$ for $\hat{a}_x < lb_1$ and at $g(\hat{a}) = a_{ref1}$ if $\hat{a} \geq ub_1$ and varies linearly in between. Here a_{ref1}, ub_1 and lb_1 are model parameters, with a_{ref1} representing a comfort threshold of the driver. The fourth parameter is the coast-down acceleration, a_0, and is accounted for by the mechanical properties of the vehicle: rolling resistance, engine brake torque and aerodynamic drag. This is determined by the following polynomial function:

$$a_0(U) = c_1 + c_2 U + c_3 U^2 \qquad (4)$$

with parameter values determined from representative vehicle data: $c_1 = -105.2\,\mathrm{ms}^{-2}$, $c_2 = -16.70\,\mathrm{s}^{-1}$, $c_3 = -0.4789\,\mathrm{m}^{-1}$. For the turn stage (Fig. 3(b)), a modified input is used, $\max(\hat{a}, a_y)$; this allows the driver to apply additional braking if the magnitude of the instantaneous lateral acceleration a_y exceeds the lower threshold. The thresholds are biased to higher values, starting at ub_2, since it is only if the entry speed was too high that additional braking effort need be applied.

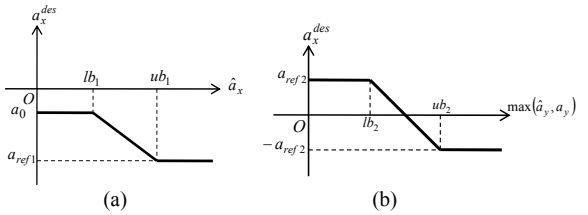

(a) (b)

Fig. 3. Nonlinear control function $g(.)$ for the approach stage (a) and turn stage (b).

For completeness, a speed control model is supplied for the recovery-stage, but this is not a primary focus of this paper; in fact $\hat{a}$ and a_y both tend to zero as the vehicle completes the turn, so other driver attributes must be active in this third stage. Also, this stage has minimal influence on the conflict metrics mentioned in Section I. We assume a simple proportional controller based on a desired target speed

$$a_x^{des} = a_{ref3}\,. \qquad (5)$$

All initial conditions for simulation (position, speed and acceleration) were obtained directly from the driving data at the start time of the chosen event.

III. INVESTIGATION OF $\hat{a}$ USING DRIVING DATA

In this section the full speed control model of Fig. 2 is not used; rather, the reference $\hat{a}$ is computed directly from the naturalistic driving data to test whether it is reasonably well controlled by the human driver.

A. Data Source

The events analyzed in this study were obtained from a pre-existing naturalistic driving database from the University of Michigan Transportation Research Institute (UMTRI) [15]. The subjects in that study drove instrumented vehicles, provided for approximately one month, as substitutes for their personal cars. Thus, the control behavior shown by these drivers is considered typical of normal driving, and not biased by experimental protocols. The trajectories were derived from differential GPS measurements fused with on-board motion sensors by use of Kalman filters [5].

B. Braking to Rest

Fig. 4 shows a comparison between $\hat{a}$ (or equivalently $\hat{a}_x$ for straight driving case) and the longitudinal acceleration of the vehicle, a_x, for an event of braking to rest at the stop bar for a red traffic signal. In this example case, the braking period started when $\hat{a}$ reached around 1.45 m/s^2 and was regulated between an upper bound (1.7 m/s^2) and lower bound (1.4 m/s^2) until the vehicle speed became slow near the stop bar. These upper and lower bounds were determined as the maximum and minimum decelerations respectively between the time at brake initiation (first brake application) and a point 5 m before reaching the stop bar. The last 5 m before final stopping was not considered, since the driver strategy is most likely based on position control and the vehicle speed becomes very small (less than 3 m/s for this event). It is especially important to note that while the reference $\hat{a}$ is well controlled, within tight limits, the actual vehicle acceleration fluctuates considerably. This suggests that $\hat{a}$ is a plausible control reference, while other dynamics (included in Fig. 2) generate significantly different vehicle response, and certainly not a constant deceleration. It is noted that, although the braking initiation needs to occur within the range of comfortable acceleration, the maximum (minimum)

of $\hat{a}$ in Fig. 4 is not the same quantity as one of the model parameters lb_1 (ub_1) in Fig. 3.

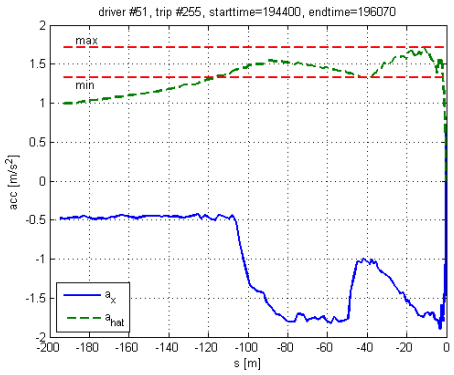

Fig. 4. a_x and $\hat{a}$ for an event of braking to rest.

C. Free Left Turn at Intersection

For a chosen left turn event, Fig. 5 shows an aerial photo of the intersection and the measured vehicle trajectory; video review confirmed the absence of other traffic etc. that might bias the speed control. The circle shows the first gaze point for $\hat{a}_x$, and the triangle is the second gaze point for $\hat{a}_y$ located next to the stop bar.

(a)

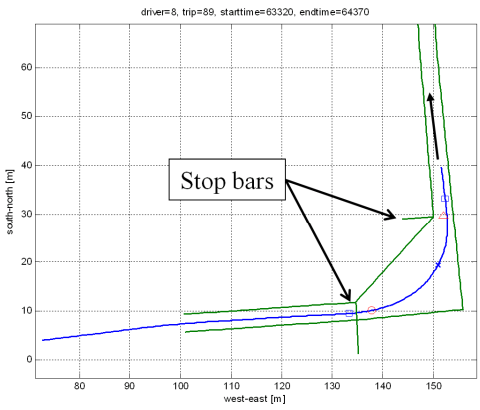

(b)

Fig. 5. Aerial photo of the example intersection (a) and free turn vehicle path with the path boundaries (b). (○: first gaze point, △: second gaze point, ×: point of maximum curvature)

Fig. 6 shows the traces of a_x, a_y, $\hat{a}_x$ and $\hat{a}_y$ for this event. The markers are the same as for Fig. 5, with the addition of the star to show the crossover between $\hat{a}_x$ and $\hat{a}_y$. The approach stage in a left turn is based on the exactly same model as the braking-to-rest event as shown by $\hat{a}_x$. It can be confirmed that the trend in $\hat{a}_x$ is very similar to that in Fig. 4 for the event of braking to rest, i.e. $\hat{a}_x$ saturates at about the actual deceleration value. Since the driver is presumed to respond to the smaller prior acceleration estimate ($\hat{a}_x$ or $\hat{a}_y$), it is necessary to compute both. As seen in the figure, in the approach stage, $\hat{a}_x$ is used for the speed control until the crossover is reached at $s = 53$ m, which corresponds to the timing of releasing the brake pedal. Then, the "threat" from $\hat{a}_y$ becomes lower than that from $\hat{a}_x$ and the turn stage starts with the speed control based on $\hat{a}_y$. Finally, the recovery stage begins at the × located at about $s = 82$ m. In the figure, $\hat{a}_x$ and $\hat{a}_y$ become indeterminate close to their respective gaze points, and the computation shows this tending to infinite values; neither case affects the control and for convenience the limit value show as $\hat{a}_x = 0$.

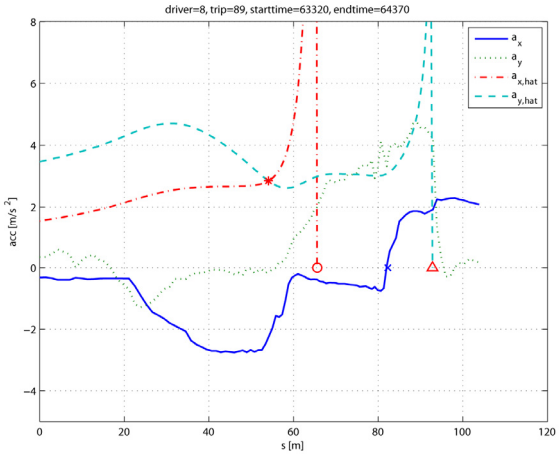

Fig. 6. a_x and $\hat{a}$ for a left turn event.

IV. EXAMPLE SIMULATIONS

Here the full speed control model of Fig. 2 is applied to example events, including parameter optimization. The MATLAB function *fminsearch* was used to minimize the error squared between the speed responses from the simulation and driving data. Two examples are presented for each of braking to rest and left turn cases.

A. Braking to Rest at Stop Bar

Resulting parameter values are given in Table I, and resulting plots are shown in Figs. 7 and 8. The horizontal lines in Figs. 7(a) and 8(a) specify the locations of *ub* and *lb*. Here *ub* and *lb* are the model parameters of Section II, and are not expected to coincide with upper and lower bounds of Fig. 4. Here only one speed control mode exists, i.e. the approach stage, so Table I comprises a reduced set of parameters. As

shown in the figures, the model can fit the data very well. In these results, $\hat{a}$ is controlled around 1.5 m/s^2 and 1.1 m/s^2 respectively until the release of the brake pedal is initiated. As shown in Fig. 8(c), this period cannot be described by the presented speed control model which is intended to regulate $\hat{a}$ within a desired range and therefore another mechanism must be dominant in this region. However, as mentioned previously, this region is not significant to the driver threat since the vehicle speed is low.

TABLE I
DRIVER PARAMETERS FOR BRAKING TO REST

Symbol	Quantity	Value	
		Ex. 1	Ex. 2
K [s^{-1}]	proportional gain	0.723	0.873
ub_1 [m/s^2]	upper bound of the desired $\hat{a}$ range	1.47	0.993
lb_1 [m/s^2]	lower bound of the desired $\hat{a}$ range	1.19	0.840
$a_{ref\,1}$ [m/s^2]	lower saturation value of the saturation block	−1.66	−1.09

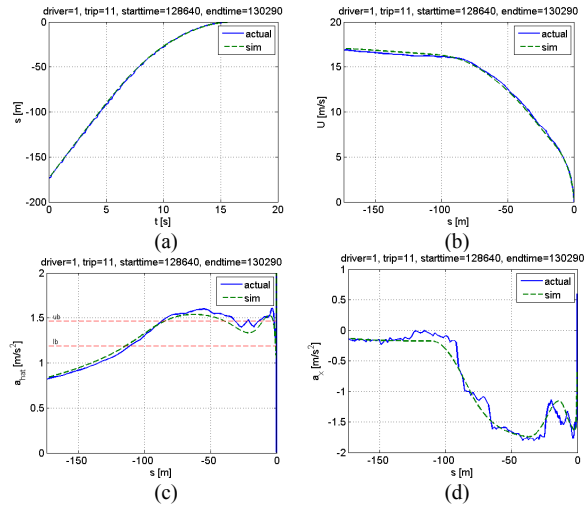

Fig. 7. Simulation results for braking to rest (Example 1).

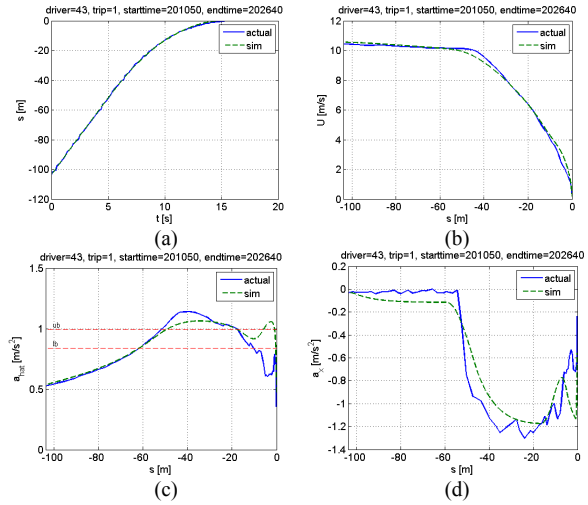

Fig. 8. Simulation results for braking to rest (Example 2).

B. *Left Turn Across Path*

Results of optimization and simulation are shown in Figs. 9 and 10; they show the model can reproduce the left turn motion accurately. Corresponding parameter values for this example are given in Table II.

Here, the gaze points are fixed at the locations defined in Section II, meaning that the fixed assumed relationship between the road geometry information and driver's attention was employed. This affects the mode switching point from the approach stage to turn stage. A relatively large undershoot shown in Fig. 10(b) seems due to a slight mismatch between the predicted and actual switching timings. Nevertheless, the speed control can compensate the error reasonably quickly. The error in speed is small for conflict metrics (i.e. PET and LB/TB). For example, if an average error of −0.5 m/s from a nominal speed of 7 m/s lasts for 10 m, the error in time is only $10\times(1/6.5-1/7)=0.11$ s.

TABLE II
DRIVER PARAMETERS FOR LEFT TURNS

Symbol	Quantity	Value	
		Ex. 3	Ex. 4
K [s^{-1}]	proportional gain	2.18	2.18
ub_1 [m/s^2]	upper bound of the desired $\hat{a}_x$ range	2.85	2.62
lb_1 [m/s^2]	lower bound of the desired $\hat{a}_x$ range	1.85	1.62
ub_2 [m/s^2]	upper bound of the desired $\hat{a}_y$ range	3.46	3.11
lb_2 [m/s^2]	lower bound of the desired $\hat{a}_y$ range	2.46	2.11
$a_{ref\,1}$ [m/s^2]	lower saturation value of the saturation block (approach stage)	−3.14	−2.77
$a_{ref\,2}$ [m/s^2]	saturation value for the turn stage	0.602	0.748
$a_{ref\,3}$ [m/s^2]	constant desired acceleration for the recovery stage	2.98	1.49

Regarding the parameter values, those in Table II are significantly larger than those in Table I, but the events are under different conditions. Clearly, the measured vehicle decelerations are larger in the left turn events than in the braking-to-rest events, suggesting different control patterns are employed for different conditions; for example it can be that the sense of urgency or risk are very different. Another factor may be the need for precise positioning, which is probably greater in straight-line braking. Even though the parameters may vary, the mechanisms appear consistent between these situations.

V. CONCLUSIONS

The objective of this paper was to model speed control at intersections, with special emphasis on the approach stage before turning takes place. It was seen that a prior acceleration estimate $\hat{a}$ can be used as reference signal for a

speed control model of human drivers negotiating intersection left turns. The resulting model performance, shown through a limited number of simulation results, is highly promising and confirms the feasibility of the model.

Future development will combine the speed controller with a lateral control model, giving an integrated driver model for turning behavior at intersections under free-flow conditions.

Model parameters define characteristics of the driver, and the values of such parameter clearly vary between different drivers and different events. Therefore, a further goal of future research is to analyze larger numbers of events, and hence characterize frequency distributions of model parameters, potentially related to factors such as driver style, age and gender. Response to other traffic in the vicinity of the turn, particularly for gaps in oncoming traffic, is another challenging goal for future model development. Further aspects of modeling may require automated techniques, such as evolutionary algorithms [18].

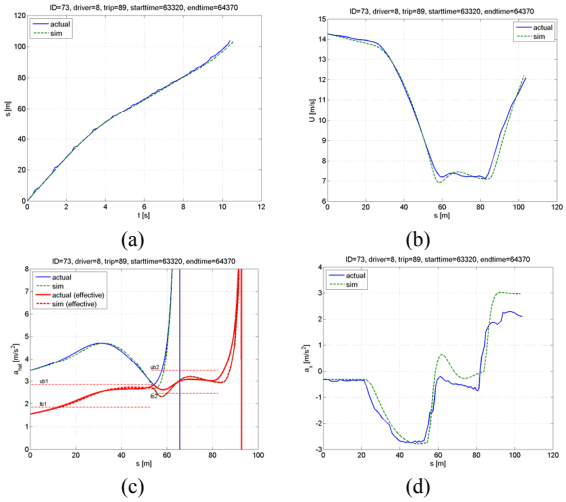

Fig. 9. Simulation results for left turn (Ex. 3).

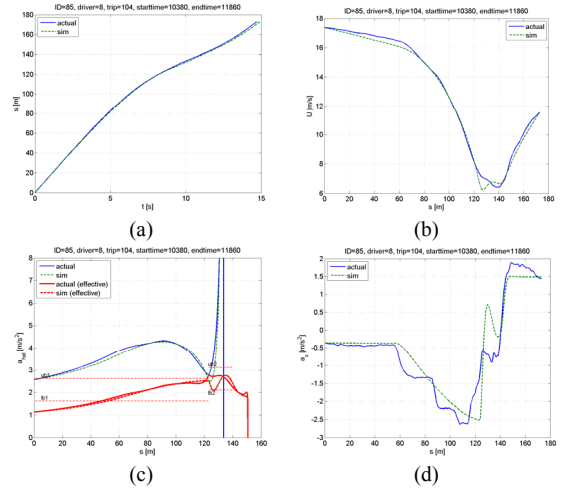

Fig. 10. Simulation results for left turn (Ex. 4).

REFERENCES

[1] B.L. Allen, T.T. Shin and P.J. Cooper, "Analysis of Traffic Conflicts and Collisions," Transportation Research Record, vol. 667, pp. 67-74, 1978.

[2] D. Gettman and L. Head, "Surrogate Safety Measures from Traffic Simulation Models," Federal Highway Administration., Tech. Rep. FHWA-RD-03-050, 2003.

[3] J.A. Misener, C.Y. Chan, D. Cody, S. Dickey, C. Nowakowski, D. Greenhouse, D. Ragland, S.E. Shladover and J. Vanderwerf, "California Intersection Decision Support: A Systems Approach to Achieve Nationally Interoperable Solutions II," California Partners for Advanced Transit and Highways., 2007.

[4] C.Y. Chan, "Characterization of Driving Behaviors Based on Field Observation of Intersection Left-Turn Across-Path Scenarios," IEEE Transactions of Intelligent Transportation Systems, vol. 7, pp. 322-331, 2006.

[5] K. Nobukawa, M. Barnes, R. Goodsell and T. Gordon, "Reconstruction of Vehicle Trajectories for Intersection Conflict Analysis Using Vehicle-Based Sensors," in International Association for Vehicle System Dynamics, 2009.

[6] C.C. MacAdam, "Understanding and Modeling the Human Driver," Vehicle System Dynamics: International Journal of Vehicle Mechanics and Mobility, vol. 40, pp. 101, 2003.

[7] C.G. Drury, "Movements with Lateral Constraint," Ergonomics, vol. 14, pp. 293, 1971.

[8] D.J. Bottoms, "The interaction of driving speed, steering difficulty and lateral tolerance with particular reference to agriculture," Ergonomics, vol. 26, pp. 123-139, 1983.

[9] K. DeFazio, D. Wittman and C.G. Drury, "Effective vehicle width in self-paced tracking," Appl.Ergon., vol. 23, pp. 382-386, 12. 1992.

[10] C. Coutton-Jean, D.R. Mestre, C. Goulon and R.J. Bootsma, "The role of edge lines in curve driving," Transportation Research Part F: Traffic Psychology and Behaviour, vol. 12, pp. 483-493, 11. 2009.

[11] A. Taragin, "Driver Performance on Horizontal Curves," in Proceedings of Highway Research Board, pp. 446-466, 1954.

[12] J. Emmerson, "Speeds of Cars on Sharp Horizontal Curves," Traffic Engineering and Control, vol. 11, pp. 135-137, 1969.

[13] G. Reymond, A. Kemeny, J. Droulez and A. Berthoz, "Role of Lateral Acceleration in Curve Driving: Driver Model and Experiments on a Real Vehicle and a Driving Simulator," Human Factors: The Journal of the Human Factors and Ergonomics Society, vol. 43, pp. 483-495, January 1. 2001.

[14] J.H. Hogema, "Effects of rain on Daily Traffic Volume and on Driving Behaviour," TNO., Tech. Rep. TM-96-B019, 1996.

[15] D. LeBlanc, J. Sayer, C. Winkler, R. Ervin, S. Bogard, J. Devonshire, M. Mefford, M. Hagan, Z. Bareket, R. Goodsell and T. Gordon, "Road Departure Crash Warning System Field Operational Test: Methodology and Results, Volume 1: Technical Report," National Highway Traffic Safety Administration., Tech. Rep. UMTRI-2006-9-1, 2006.

[16] W.H. Levison, B.H. Kantowitz, M.J. Moyer and M. Robinson, "A Stopping-Distance Model for Driver Speed Decision Making in Curve Approach," in Human Factors and Ergonomics Society Annual Meeting Proceedings, pp. 1222-1226, 1998.

[17] D.N. Lee, "A Theory of Visual Control of Braking Based on Information about Time-to-Collision," Perception, vol. 5, pp. 437-459, 1976.

[18] Jian-Lin Wei, Jihong Wang and Q.H. Wu, "Development of a Multisegment Coal Mill Model Using an Evolutionary Computation Technique," Energy Conversion, IEEE Transactions on, vol. 22, pp. 718-727, 2007.